Environ. Sci. Technol. **2002**, *36,* 3234−3241

Determination of Longitudinal Dispersion Coefficient and Net Advection in the Tidal Hudson River with a Large-Scale, High Resolution SF_6 Tracer Release Experiment

DAVID T. HO,*,† PETER SCHLOSSER,†,‡,§ AND THEODORE CAPLOW‡

Lamont-Doherty Earth Observatory of Columbia University, Palisades, New York, 10964, Department of Earth and Environmental Engineering, Columbia University, New York, New York 10027, and Department of Earth and Environmental Sciences, Columbia University, New York, New York 10027

Physical processes such as advection, dispersion, and air−water gas exchange play important roles in determining the movement and change in concentration of contaminants discharged into rivers. In the following, we report results from a large-scale SF_6 tracer release experiment conducted in the tidal Hudson River to examine longitudinal dispersion and net advection. SF_6 was injected into the Hudson River near Newburgh, NY, and surveyed for 13 days using a new, fully automated, high-resolution SF_6 sampling and analysis system. Net down river advection of the water body originally tagged with SF_6 was slow, averaging mean displacement rates of about 0.5 ± 0.2 km d^{-1}. In contrast, spreading of the tracer was driven by tidal movement, causing rapid mixing of the water up and down river. By examining the change in the second moment of the tracer distribution with time, we determined the mean longitudinal dispersion coefficient to be 70.1 ± 4.3 m^2 s^{-1}. Temporal evolution of the SF_6 inventory indicates an average gas transfer velocity over the period of the experiment of 6.5 ± 0.5 cm h^{-1} (1.56 ± 0.12 m d^{-1}). Vertical profiles show that mixing into the bottom layers of the river, in places reaching more than 53 m, seemed to be rapid.

Introduction

One critical element in designing management strategies for rivers is understanding of the dynamics of perturbations introduced into the water. Such perturbations include climatically forced variables (e.g., changes in freshwater runoff) as well as spills of contaminants related to human activities along the river or in its watershed. For example, toxic contaminants could enter rivers by a variety of methods, including industrial and municipal wastewater discharges, urban runoff, accidental spills, landfill leachate, and tributary discharges. After the initial discharge, physical processes such as advective transport and dispersion play important roles in determining the movement and change in concentration of contaminants. Thus, they influence decision on methods used for detection, remediation, and treatment that are likely to be most successful. Whereas local rates of mean advection can be estimated from streamflow and river channel geometry, longitudinal dispersion is more difficult to determine *(1, 2)*. A large disparity exists between the values of dispersion coefficients obtained for idealized and real systems, with experiments in simplified systems (such as irrigation canals) appearing to grossly underestimate the dispersion that occurs in rivers *(2)*. Such a disparity suggests that the processes contributing to dispersion in rivers are not well understood. Yet, the fact that advection and dispersion are fundamental variables for evaluation of water quality in aquatic systems by conceptual or numerical models implies that better understanding of these processes is necessary for the continued improvement of such models. To further understanding of these processes, a number of field experiments have been conducted.

Generally, these field experiments have used fluorescent dyes as tracers *(3−5)* because they can be easily measured in the field over concentration ranges of several orders of magnitude using portable fluorometers, and their background concentrations in most natural waters are very low *(6)*. However, for long-term and large-scale experiments, fluorescent dyes are not ideal tracers because both laboratory and field experiments have demonstrated that most of them are not conservative in natural waters *(3, 4, 6)*, degradation products of some dyes, such as Rhodamine WT, can be toxic *(7)*, and they are relatively expensive. As an alternative, Clark et al. *(8)* demonstrated the potential of SF_6 as a tracer for determining longitudinal dispersion in large rivers during a pilot experiment. SF_6 shares many of the characteristics that make fluorescent dyes successful tracers in rivers, while at the same time being detectable over a larger concentration range as well as being less expensive. Together, these properties provide SF_6 with advantages over fluorescent dyes in that tracer experiments can be conducted over larger spatial and time scales in rivers and at a much lower cost compared to fluorescent dyes. Furthermore, SF_6 differs from fluorescent dyes in that it is a gas. Thus, its loss from solution across the air−water interface to the atmosphere can be used to determine the gas transfer velocity (i.e., reaeration coefficient), either by simultaneously injecting another gas (e.g., ^3He) or by calculating a mass balance.

Our previous SF_6 experiments conducted in the Hudson River *(8−10)* suffered from the fact that discrete samples for SF_6 analysis had to be collected using Niskin bottles and a small winch installed on the boat and then transferred to 50 mL glass syringes for analysis, thus significantly degrading the resolution compared to fluorescent dye experiments. In the present study, we significantly improved the resolution by using a fully automated, high-resolution SF_6 sampling and analysis system. In the following, we report results from a large-scale SF_6 tracer release experiment conducted in the tidal Hudson River near Newburgh, NY, in July/August 2001 to examine advection and longitudinal dispersion.

Study Location

The Hudson River originates from Lake Tear of the Clouds on Mount Marcy in the Adirondacks. From there, the river flows in a southerly direction for 510 km into New York Harbor and drains an area of approximately 35 000 km^2 *(11)*. More than 95% of the drainage basin is in New York State, and the

* Corresponding author phone: (845)365-8706; fax: (845)365-8155; e-mail: david@ldeo.columbia.edu.

† Lamont-Doherty Earth Observatory of Columbia University.

‡ Department of Earth and Environmental Engineering, Columbia University.

§ Department of Earth and Environmental Sciences, Columbia University.

10.1021/es015814+ CCC: $22.00
Published on Web 06/20/2002

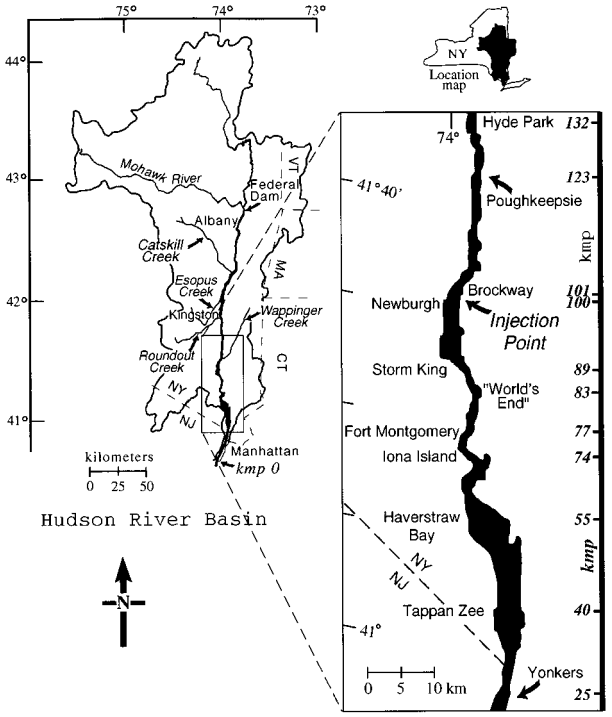

FIGURE 1. Map of the Hudson River showing location of the SF_6 tracer release experiment.

remainder lies in New Jersey, Vermont, Massachusetts, and Connecticut. For nearly half of its journey, from the Federal Dam at Troy, NY (kmp 248; locations along the Hudson River are referred to by the axial distance or kilometer point (kmp), from the Battery at the southern tip of Manhattan) to the Battery, the Hudson is a tidal river (Figure 1).

Of the total freshwater discharge into the tidal Hudson River, 50−80% enters at the Federal Dam. Contributions from four large tributaries between the Federal Dam and Newburgh (kmp 100), Wappinger Creek (kmp 108), Rondout Creek (kmp 148), Esopus Creek (kmp 166), and Catskill Creek (kmp 183) account for most of the remaining freshwater discharge. Flow at the Federal Dam varies seasonally, with maximum (>800 $m^3\ s^{-1}$) and minimum (50−200 $m^3\ s^{-1}$) mean daily flows occurring during spring and late summer, respectively. The position of the saltwater/freshwater interface also varies seasonally, depending on freshwater runoff. Typically, during high spring runoff associated with snowmelt, it is located between Yonkers and the Tappan Zee (kmp 25−40), and during low runoff in late summer it is positioned near Newburgh (kmp 100).

The SF_6 tracer release experiment was performed in a stretch of the tidal Hudson River from Yonkers to Hyde Park (kmp 29−132). SF_6 was injected into the river near Newburgh (kmp 100), and the center of the tracer patch, defined as water with SF_6 concentration greater than 5% of the maximum SF_6 concentration measured that day, was confined to a 24 km reach of river between Fort Montgomery and Brockway (kmp 77 and 101). Here, the axis of the river has a north−south trend with several significant bends in the river (Figure 1). There are two areas, located near Storm King (kmp 89) and World's End (kmp 83), where the bottom deepens significantly (dead zones). The bottom depths at these two locations are about 26 and 53 m, respectively.

Extensive areas of shallow water (<2 m) along the shore, between kmp 88 and 98, further add to the complexity of the geometry. The cross-sectional area of the channel does not vary much along this reach (Figure 2), although the mean depth and width of the channel change significantly. The mean depth varied between 6 and 33 m and averaged about

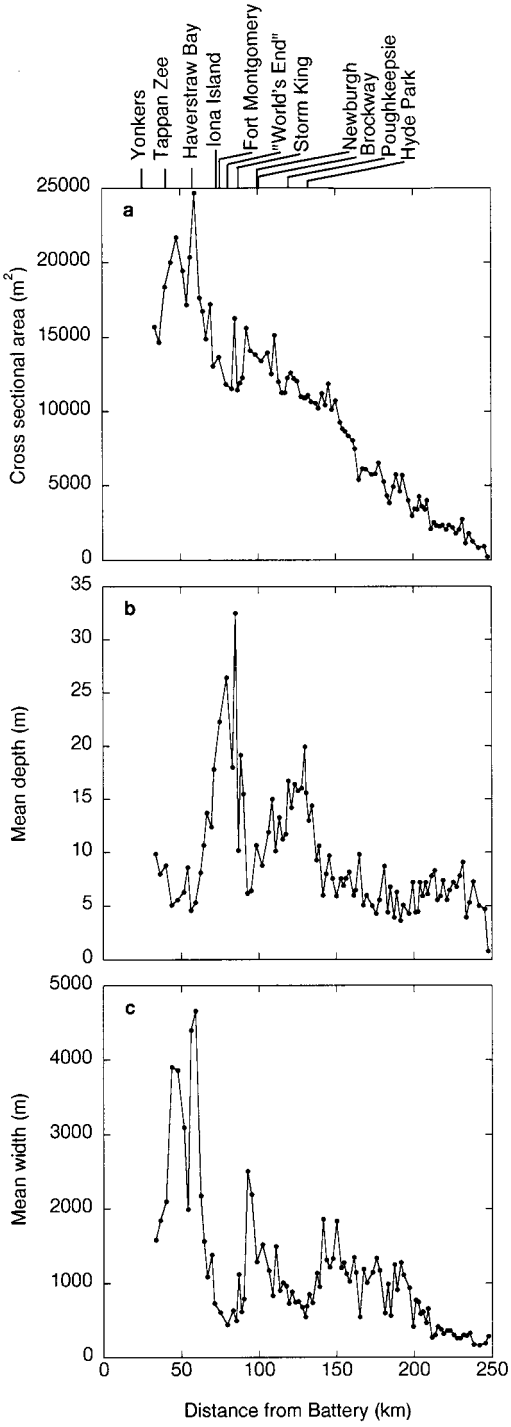

FIGURE 2. Hudson River geometry as a function of distance from the Battery at the tip of Manhattan.

17 m (Figure 2), and the mean width varied between 450 and 2500 m and averaged about 1000 m (for more detailed information on the Hudson River geometry, see Supporting Information**)**. No major tributaries enter along this stretch of river. During the 2-week experiment, the mean freshwater discharge rate over the Federal Dam was 132 ± 16 $m^3\ s^{-1}$, within the range of the climatological low for the summer period, and surface water temperature along the river varied from about 26 to 28 °C.

Experimental Section

Tracer Injection. On July 25, 2001, ca. 4.3 mol of SF_6 were injected from a boat into the river off Newburgh, NY, north

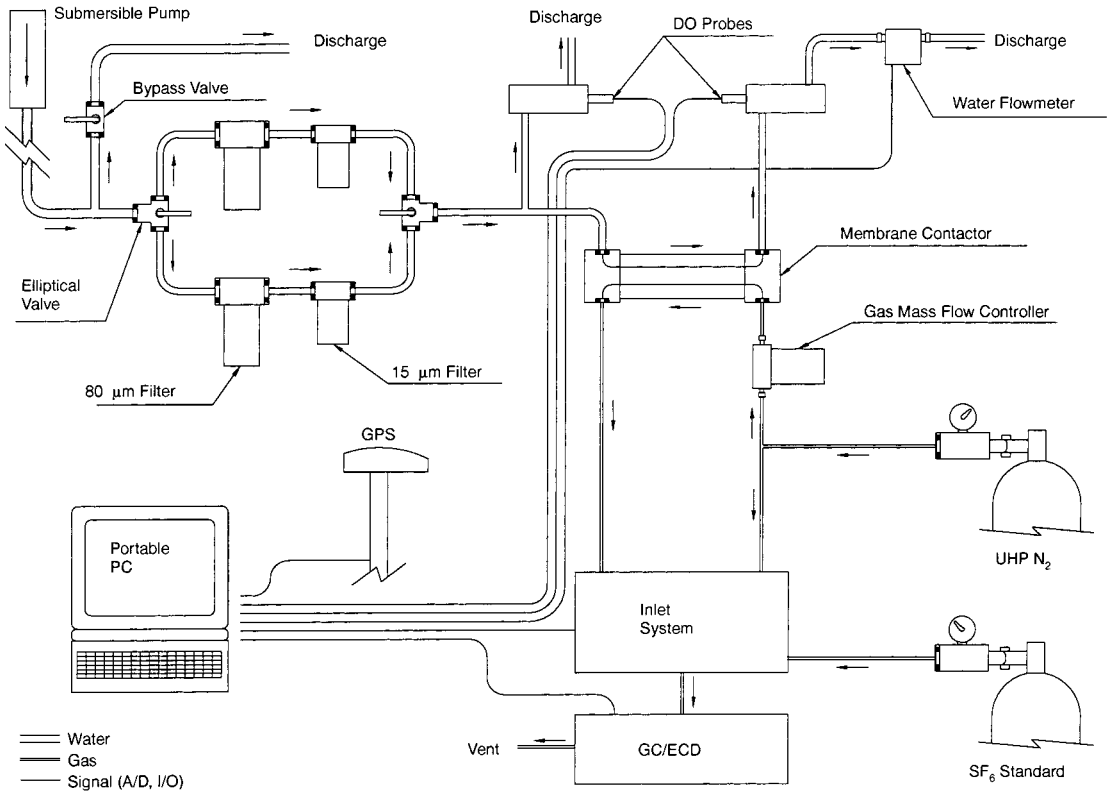

FIGURE 3. Schematic diagram of fully automated, high-resolution SF_6 analysis system.

of the Newburgh-Beacon Bridge. Based on subsequent SF_6 measurements, it was calculated that 1.1 mol of SF_6 originally injected as gas bubbles dissolved in the water. The injection device consisted of 7 m of diffusion tubing (0.6 cm I.D.; rubber and polyethylene; nominal pore size: 150 μm) curled around an aluminum cylinder attached to a lead weight. Over a period of about 20 min, as the boat twice traversed the channel perpendicular to the main axis of the river, SF_6 was injected at depth to ensure rapid transverse and vertical mixing. The injection device was attached to a 9 m long rope. However, because of drag caused by the rope and injection device, the injection line was towed at an angle of about 45°, resulting in an injection depth of approximately 5 m.

Fully Automated Continuous SF_6 Analysis System. SF_6 was monitored continuously from a boat (RIVERKEEPER) by pumping water (intake: ≈2 m depth) via a submersed pump (Grundfos 5SQE03A-90) mounted on the front of the boat, through a length of reinforced PVC hose and into a gas extraction unit, followed by analysis using an onboard gas chromatograph (see Figure 3). The measurement interval was 2 min.

The gas extraction unit consisted of a series of filters, a membrane contactor (Liqui-Cel), two dissolved oxygen (DO) sensors, and gas and water flow controllers and flow meters. During operation, water was pumped through two stainless steel mesh filters (80 and 15 μm, respectively) mounted in series and into the membrane contactor. The membrane contactor contains thousands of microporous (0.05 μm) polypropylene hollow fibers. Water pumped from the Hudson River flowed over the outside of the hollow fibers, while ultrahigh purity (UHP; 99.999%) N_2 flowed countercurrent on the inside of the hollow fibers, resulting in rapid transfer of dissolved SF_6 from the liquid phase to the gas stream. DO meters were situated in the water stream before and after the membrane contactor to measure the DO extraction efficiency. This value was used to calculate the SF_6 extraction efficiency, applying a relationship between DO and SF_6 extraction efficiencies determined in the laboratory. During the experiment, SF_6 extraction efficiency varied between 40 and 60% and averaged 50% for the entire period. Uncertainty in the relationship between DO and SF_6 extraction efficiency contributed an uncertainty of the order of ±5% to the calculated SF_6 concentrations. However, since any error in this relationship would lead to a systematic offset in the calculated SF_6 concentrations, most of the calculations presented here were unaffected because knowledge of absolute SF_6 concentrations is not necessary for estimation of advection and dispersion rates.

To express SF_6 as molar concentration of SF_6 per volume of water, the difference in the water flow rate (2 L min^{-1}) and the N_2 flow rate (100 mL min^{-1}) needs to be taken into account. This was done by scaling the calculated SF_6 concentrations by the flow rates. N_2 flow rate was maintained by an electronic mass flow controller, whereas water flow rate from the pump was regulated by adjusting a ball valve on the flow bypass. When the water flow rate dropped below a certain threshold, the elliptical valves were switched, and the other set of filters was used.

At two minute intervals, the gas stream was diverted through a physical (Nafion) and a chemical ($Mg(ClO_4)_2$) dryer before filling a sample loop. Subsequently, the sample was injected into a gas chromatograph (GC) equipped with an electron capture detector (ECD) by UHP (99.999%) N_2 carrier gas. The SF_6 was separated from other gases at room temperature with a molecular sieve 5A column. Typically, 10 samples were bracketed by standards. During data reduction, the sample concentrations were calculated from time-weighted standards. Three different sample loops were used during the experiment (0.12, 0.62, and 1.52 mL) to increase the dynamic range of the SF_6 measurements. The analytical precision, based on repeated measurements of the standard, was ±5%, ±1%, and ±1% for the 0.12, 0.62, and 1.52 mL loops, respectively.

Valve control and data acquisition were handled by a combination of hardware and software (LabView) running on a portable personal computer. The hardware was con-

nected to the computer via Universal Serial Bus (USB) and contains digital input/output (I/O) ports and 24-bit analogue to digital (A/D) data acquisition ports. In addition to the signal from the GC-ECD, the A/D also acquired signals from the water flow meter. Communication with the global positioning system (GPS) and the two DO meters were accomplished via RS-232 serial ports on the computer. During each analysis, the analogue output of the GC-ECD was converted to a digital signal by the data acquisition board and analyzed by a commercially available chromatography package (WillStein). The results were stored on the computer.

During the experiment, the maximum boat speed was about 15 km h^{-1}, whereas the average speed was about 4 km h^{-1} for the first day and 12 km h^{-1} thereafter. Spatial resolution of the measured tracer distributions, 0.13 km for the first day and 0.4 km thereafter, is determined by the measurement interval and the speed of the boat. On the first day after the injection, the SF_6 patch was only 25 km wide, while the center of the patch covered only 4 km. However, a spatial resolution of 0.13 km would still provide 28 data points to resolve the shape of the peak. After the first 2 days, when the center of the patch grew to more than 10 km, a spatial resolution of 0.4 km provided an adequate number of samples to resolve the shape of the peak. At the end of the experiment, when the tracer patch covered more than 100 km of the river, it took more than 8 h to complete a transect. At this point, the boat speed started to limit the survey capability. In the future, decreasing the time needed for each analysis would enable the boat speed to be increased while maintaining the same spatial resolution. This modification would allow for greater sampling resolution after the initial tracer injection as well as for increased spatial coverage.

Because of the residence times of N_2 and water in the gas and water streams, respectively, there was a lag time of about 1 min between the time when the computer acquired time and position information from the GPS and the time when the SF_6 was actually extracted from the water. However, the lag has not been corrected for because such a correction depends on the speed of the boat and therefore is variable throughout the experiment. At an average boat speed of 12 km h^{-1}, this lag corresponded to an offset of only about 0.2 km.

The system seemed to exhibit a "memory" effect, which manifested itself either when it encountered very high SF_6 concentrations followed by a rapid decline or at very low SF_6 concentrations. The former situation only occurred on the day of the injection, when the tracer patch was surveyed hours after the injection and the concentrations exceeded 70 pmol L^{-1}. The data collected during that day were not used in the current analysis. The latter situation occurred at the edge of the patch each day, making the tails of the daily tracer distribution longer than they actually were, causing the size of the patch to be overestimated. The e-folding time (characteristic time scale) for the "memory" effect was calculated to be of the order of 5−6 min, which means that the size of the patch was overestimated by about 1 km.

Tracer Depth Profile Measurements. SF_6 depth profiles were measured by lowering a submersible pump, identical to the one used for surveying the tracer patch, and attaching it to the continuous SF_6 analysis system. The pump was lowered to a certain distance off the bottom (usually about 3 m). Sufficient time was allowed to pass to flush the system, and the water was analyzed. The pump was then raised at predetermined increments, and the procedure was repeated until the desired tracer profile was obtained.

Temperature and Salinity Profile Measurements. Temperature and salinity profiles were taken at selected locations by lowering a CTD (Sea-Bird SBE 19*plus* SEACAT Profiler) with a sampling rate of 4 Hz. The accuracies for temperature, salinity, and pressure are 0.005 °C, 0.005, and 0.35 dbar, respectively. Data were recorded and stored in the Flash RAM of the CTD and processed later on a personal computer.

Results and Discussion

Temporal evolution of the tracer distributions was measured daily for 13 days after injection. In the days following injection, due to longitudinal dispersion, the tracer-tagged water spread up and down river from an initial streak to a patch covering a stretch of more than 100 km. Each day, the boat transected the tracer patch along the navigational channel from either the southern or northern end of the patch. On certain days, SF_6 depth profiles as well as CTD profiles were taken at selected locations. The assumption that the observed and cross-sectional mean concentrations are equal is not entirely correct. Transverse surveys showed that concentrations outside of the navigational channel and near the shore were often close to half of those observed in the main channel. However, because the navigational channel typically made up 75−90% of the cross-sectional area *(12)*, the error introduced by this assumption is small.

Tidal Correction. The measured tracer distributions were corrected for tidal movement that occurred during sampling in an attempt to provide synoptic distributions. All data were corrected to the same point in the daily tidal cycle, slack water before flood at the injection point at Newburgh. Tidal current velocities, peaking between approximately 0.65 and 0.90 m s^{-1} depending upon the day, were estimated using a 1-D current model (for more detailed information on the current model, see Supporting Information). Maximum velocities calculated from the 1-D current model *(13)* were supplemented by tidal observations made from the boat during the SF_6 tracer surveys. Typically, the corrections applied for tidal movement during sampling were between 0.3 and 6.9 km. However, some measurements did not require correction and others were as large as 11 km. The model was coarse, but the associated errors (although believed to be significant in magnitude) tend to cancel over the course of the experiment with regard to their impact upon rates of advection or dispersion. This cancellation occurs because a nearly equal number of transects were measured with and against the current. The tracer distributions, corrected for tidal movement, are shown in Figure 4.

Advection. In most rivers, the major mechanism that affects the movement of dissolved pollutants is the net downstream advection. However, during the 2-week experiment, the low freshwater discharge over the Federal Dam and from the other four main tributaries prevented rapid advection of water down river, thus enabling movement of saltwater up river (Figure 5). Consequently, net down river advection of the water body originally tagged with SF_6 was slow. Based on the position of the tidally corrected peak concentrations for each day, the net advection rate was about 0.5 ± 0.2 km d^{-1}. The decrease in SF_6 concentrations in the water column at a given point was caused mainly by air−water gas exchange and dispersion rather than by advection down river.

Longitudinal Dispersion Coefficients. Because of rapid vertical and transverse mixing relative to longitudinal mixing, most rivers can be approximated as one-dimensional systems. Dilution and first-order decay of a pulse of a nonreactive gas tracer in such a system can be described by a 1-D advection-diffusion equation *(1, 2)*

$$\frac{\partial c}{\partial t} + u\frac{\partial c}{\partial x} = K_x\frac{\partial^2 c}{dx^2} - \lambda c \qquad (1)$$

where c is the average cross-sectional concentration of the gas tracer, u is the average cross-sectional current velocity, K_x is the longitudinal dispersion coefficient, and λ is the first-order loss term due to gas exchange across the air−water

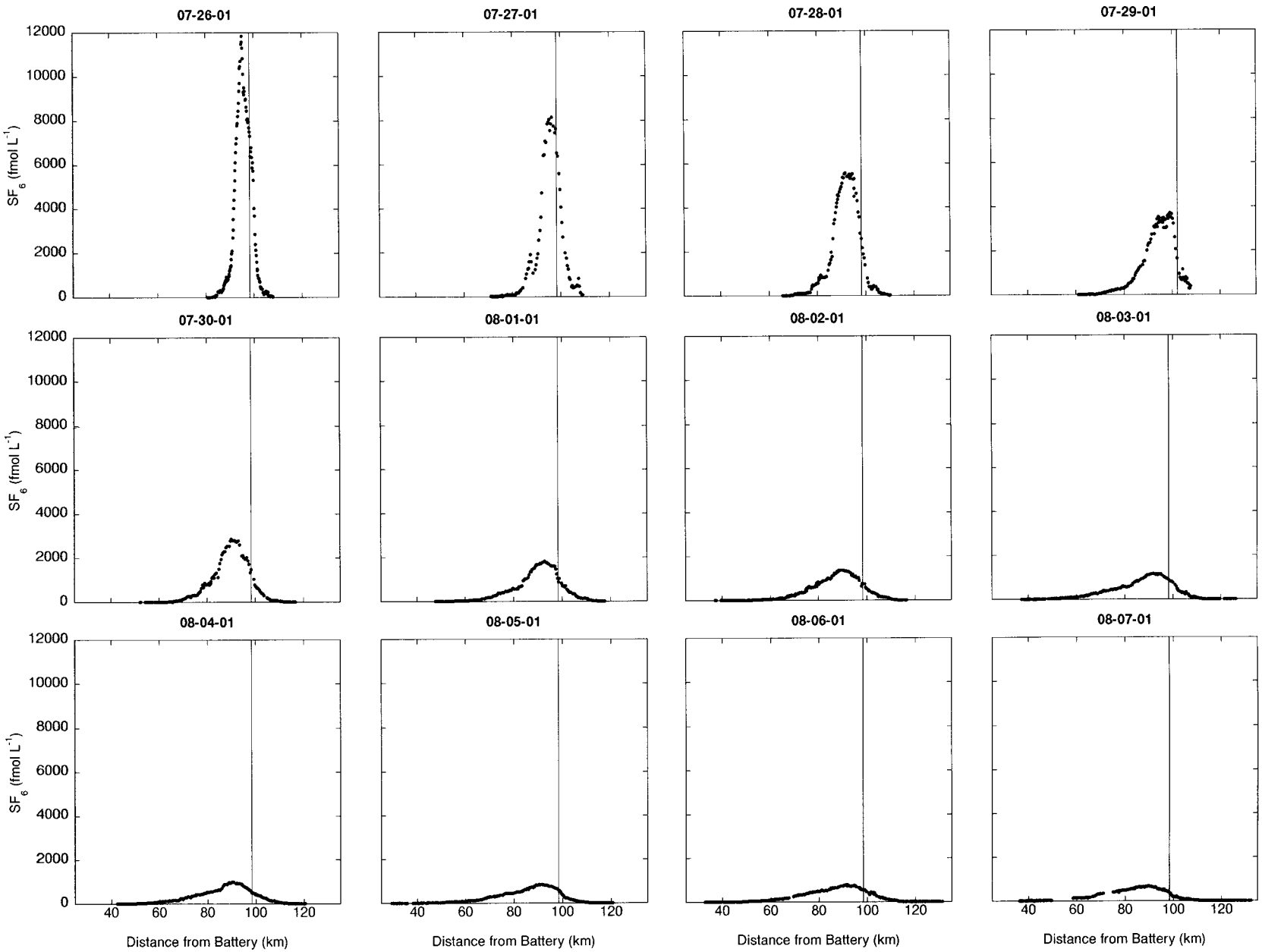

FIGURE 4. Daily SF_6 distributions. Vertical line denotes injection point near Newburgh. Distribution from July 31st is incomplete and has been omitted.

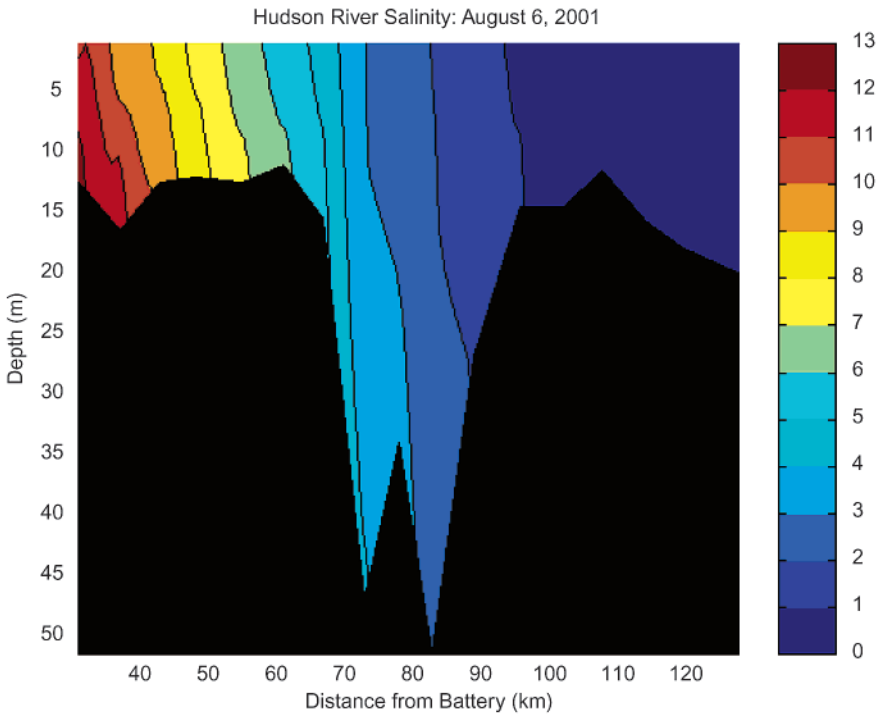

FIGURE 5. Salinity in the tidal Hudson River on August 6, 2001 as a function of distance from the Battery at the tip of Manhattan.

interface. The solution to eq 1, for an instantaneous injection of gas tracer, is

$$c(x,t) = \frac{M}{A\sqrt{4\pi K_x t}} \exp\left[-\frac{(x - ut)^2}{4K_x t} - \lambda t\right] \qquad (2)$$

where M is the mass of trace gas injected and A is the cross-sectional area of the river. One method for calculating longitudinal dispersion coefficients from experimental data is via the "change of moment" in the following manner *(1, 2)*

$$K_x = \frac{1}{2}\left(\frac{d\sigma_x^2}{dt}\right) \approx \frac{1}{2}\frac{\sigma_x^2(t_2) - \sigma_x^2(t_1)}{t_2 - t_1} \qquad (3)$$

where $\sigma_x^2(t_1)$ and $\sigma_x^2(t_2)$ are the second moments of the tracer distribution at times t_1 and t_2, respectively. σ_x^2 for each day is determined by fitting Gaussian curves to the SF_6 distributions, while minimizing chi square. Since σ_x^2 is not a perfectly linear function of time, the longitudinal dispersion coefficient, K_X, was derived by fitting a linear least-squares curve to a plot of $\sigma_x^2/2$ versus time t.

The mean longitudinal dispersion coefficient for the stretch of the river from kmp 29 to 132 over the entire 2-week experiment was calculated to be 70.1 ± 4.3 m^2 s^{-1}. This value is similar to that found by Clark et al. *(8)* (78 ± 17 m^2 s^{-1}) during the latter part (days 8−13) of a SF_6 tracer release experiment in a different part of the Hudson River in September 1994 (kmp 166 to 227). The slight difference could be due to differences in river geometry and freshwater discharge rate. These values are considerably lower than estimates derived in a previous experiment using Rhodamine B in July/August 1965, where the longitudinal dispersion coefficient near Newburgh was found to be somewhere between 92 and 269 m^2 s^{-1} *(5)*. The discrepancy between the values derived by SF_6 and Rhodamine B could be due to the fact that experiments conducted with fluorescent dyes are indicative of dispersion on a much smaller spatial scale (and on a much shorter time scale). Also, given the large

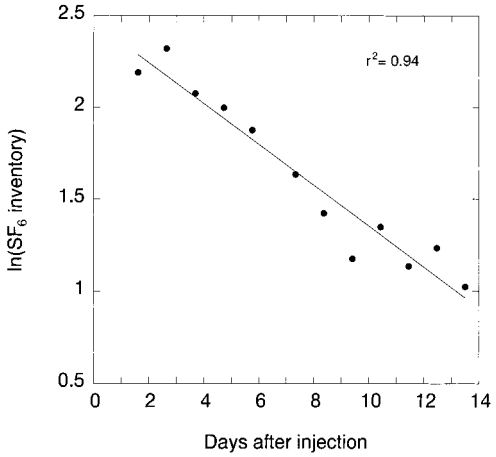

FIGURE 6. Decrease in SF_6 inventory in the tidal Hudson River as a function of time during the experiment. The point from August 3 (approx 9.5 days after injection) is an outlier and removing it from the data set does not change the results appreciably.

uncertainty in dispersion coefficients derived using Rhodamine B, it is difficult to discern what the actual value was.

As can be seen from the observed tracer distribution from the Hudson River (Figure 4), the leading edge of the tracer spreads faster and further than the trailing edge. Tracer concentration distributions often display a skewed profile due to longitudinal dispersion, even after an initial period that allows sampling of the entire flow field. This deviation from a Gaussian distribution indicates that second-order processes are contributing to the observed tracer distribution and is sometimes attributed to the initial period where the eddy diffusive length scale is large compared to the size of the tracer patch or to dead zones and other trapping mechanisms, including nonuniform channel geometry. Also, the skewed tracer distributions might be due to the uneven distribution of velocities within the tracer patch. However, analytical solutions, such as the 1-D advection-diffusion equation and its derivatives, provide Gaussian distributions and cannot predict skew. One way to determine if nonuniform

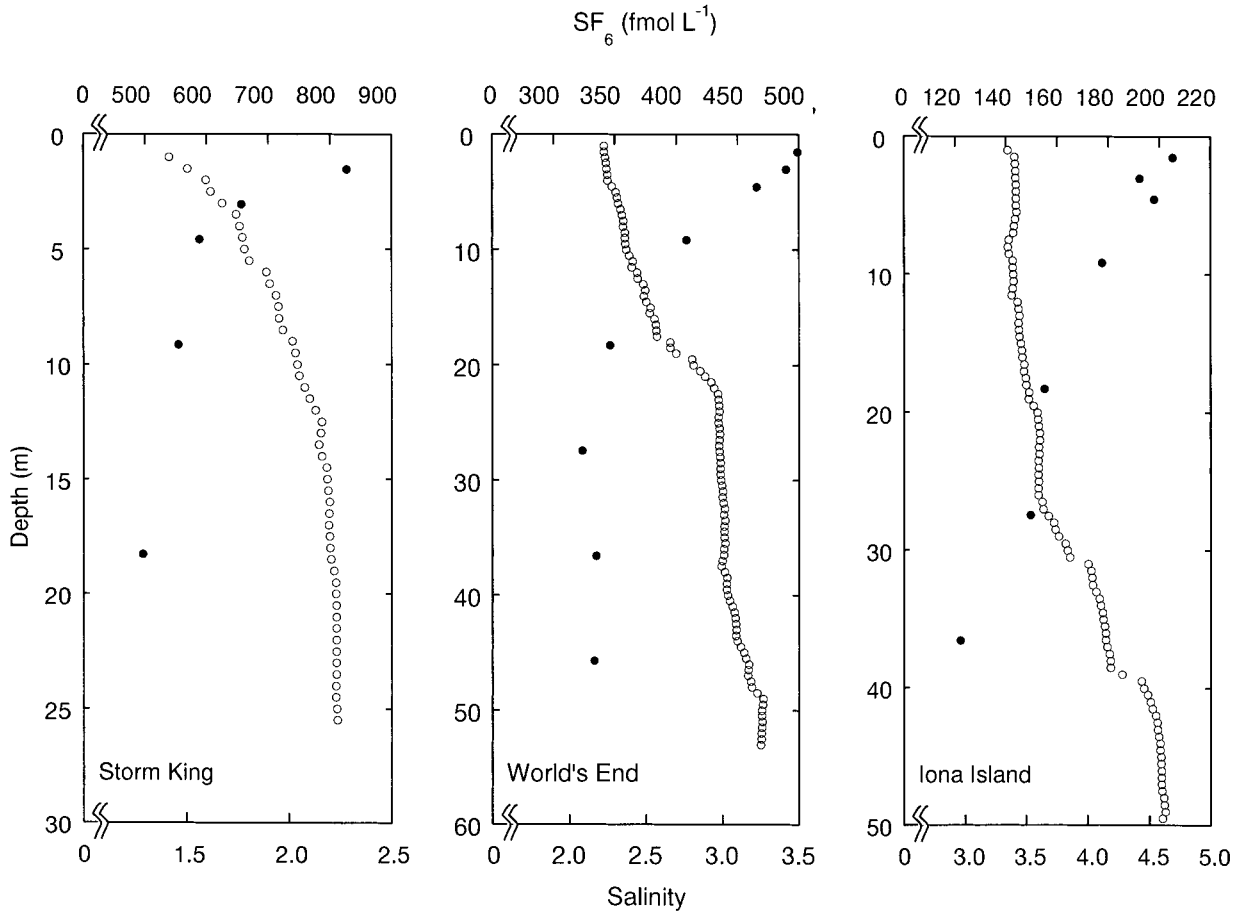

FIGURE 7. Depth profiles of SF_6 and salinity on August 2, 2001 from Storm King (kmp 89), World's End (kmp 83), and Iona Island (kmp 74). Filled circles = SF_6; open circles = salinity. SF_6 and salinity are inversely correlated, indicating mixing of saline, SF_6-free water with freshwater tagged with SF_6.

channel geometry is contributing to errors in calculations of longitudinal dispersion using eq 3 is to integrate measured SF_6 concentration over the river cross-section and to examine the resulting Gaussian distributions (see Figure E in Supporting Information). Application of this method to the tracer data leads to a decreased K_X value of 62.9 ± 4.2 m^2 s^{-1}. Finally, if the two methods are applied to the center of the tracer patch only (as defined above), the results should be less affected by the skewness as the long tails are eliminated. In this case, K_X is 65.3 ± 4.4 m^2 s^{-1} and 72.8 ± 4.7 m^2 s^{-1} for the calculation with and without considering the river cross-section, respectively. Because all of these methods yield results that are within the error estimates using eq 3, we feel that for first-order calculations, treatment of the Hudson River as a 1-D system is justified. Comparisons of other methods to calculate the dispersion coefficients based on experimental data and modeling of tracer distribution in the Hudson River is beyond the scope of this contribution and will be presented elsewhere.

Air−Water Gas Exchange. SF_6 inventories were calculated from SF_6 concentrations and the geometry of the river. The mean loss rate in SF_6 inventories was used to estimate the gas transfer velocity, k, in the following manner

$$k = \frac{F}{(c_w - \alpha c_a)} = \lambda h \qquad (4)$$

where F is the mass flux of gas across the air−water interface, c_w and c_a are the concentrations of gas in the water and in the atmosphere, respectively, α is the Ostwald solubility coefficient for SF_6 in water, and h is the mean river depth. The gas transfer velocity calculated from eq 4 was normalized to a Schmidt number Sc of 600, corresponding to values for CO_2 at 20 °C (Sc = kinematic viscosity of water divided by the molecular diffusivity of the gas in water) by assuming that k is proportional to $Sc^{-1/2}$ *(14)* as follows

$$k(600) = k_{SF_6}\left(\frac{600}{Sc_{SF_6}}\right)^{-1/2} \qquad (5)$$

where k_{SF_6} is the gas transfer velocity for SF_6, and Sc_{SF_6} is the Schmidt number of SF_6 (690 at 26.8 °C).

SF_6 inventories were calculated from river geometry data and measured concentrations, assuming lateral and vertical homogeneity such that the measured concentrations in the center of the navigational channel were assumed to be the cross-sectional mean concentrations. During the experiment, SF_6 inventories decreased exponentially (Figure 6) with a mean loss rate, λ, of 0.111 ± 0.009 d^{-1}. The mean gas transfer velocity, $k(600)$, calculated from the SF_6 loss rate, and a mean river depth of 13.1 m, is 6.5 ± 0.5 cm h^{-1}, which is higher than those calculated by Clark et al. *(9)* in 1993 and 1994 (4.4 ± 0.2 cm h^{-1} and 5.3 ± 0.2 cm h^{-1}, respectively) during two SF_6-^{3}He dual tracer release experiments in the Hudson River. Similar to the difference in longitudinal dispersion coefficients, the difference in gas transfer velocity of the various experiments could be due to differences in river geometry and river flow rate. However, as Clark et al. *(9)* observed, the relationship between gas transfer velocity and wind speed in the Hudson River is very similar to those observed previously for lakes, suggesting that wind is the primary source of near-surface turbulence in the tidal Hudson

River. Hence, differences in gas transfer velocities between the current experiment and those in 1993/1994 are most likely due to differences in wind speeds. In fact, records from a land-based station in Poughkeepsie (kmp 123) indicate that the mean wind speed over the entire experiment in 2001 was about 50% higher than those in 1993 and 1994. However, because the focus of the current experiment was not on air−water gas exchange, wind speed was not measured with the required detail, and this hypothesis cannot be verified conclusively with the present data set.

To estimate the uncertainty in calculated SF_6 inventories and gas transfer velocity due to river geometry, an additional data set of the Hudson River geometry, based on data from NOAA/NGDC, was used (F. Hellweger, personal communication, 2002). The calculated SF_6 loss rate (0.116 ± 0.009 d^{-1}), combined with the mean river depth (13.2 m), led to an estimate of the gas transfer velocity (6.8 ± 0.5 cm h^{-1}) which is similar to that estimated using the Steadfast data set.

Vertical Mixing. SF_6 depth profiles were taken near Storm King (kmp 89), World's End (kmp 83), and Iona Island (kmp 74) where the bottom depths are about 26, 53, and 49 m, respectively (Figure 7). These depth profile measurements show that mixing to great depths (>40 m) was rapid, although there was still a discernible tracer gradient between the surface and greater depths after 2 weeks. Salinity profiles from the CTD surveys show that an inverse correlation exists between salinity and SF_6 concentration (Figure 7), indicating that SF_6-tagged water at depth is being diluted by SF_6-free, saline water.

Outlook. During the experiment in July/August 2001, because of the low freshwater discharge relative to other times of the year, advection of the tracer down river was slow, and there was significant mixing of the tracer up river from the injection point. This result challenges the conventional view that pollutants discharged into a river will be advected downstream and hints at a scenario where a pollutant discharged into the river, even if it remains suspended, could linger in the river for a considerable time. As a result of slow advection, after 2 weeks, the concentration at the original injection point was still 80% of the peak concentration measured on that day. Furthermore, at the end of the experiment, SF_6 had been mixed to a part of the river 35 km upstream from the injection point.

SF_6 tracer release experiments could be designed for different scenarios, some of which cover the entire reaches of large rivers, while others target a specific region. For instance, SF_6 could be used in mixing zone studies near outfalls, where tracers could be added to wastewater outflows to establish how rapidly a wastewater stream mixes with the receiving waters. Such near-field mixing zone studies conducted with SF_6 could aid in the design of outfalls for new wastewater treatment plants and help determine the fate of substances discharged into a river before permits are granted or renewed. SF_6 could also be used to track contaminant spills, where emergency response crews may inject SF_6 at the spill site to trace the direction of net transport and magnitude of dispersion of the contaminant, which in many instances is difficult to map in a quasi-real time mode.

Further improvements could be made to the SF_6 analysis system to allow for greater survey capacity, wider areal coverage, and higher sample resolution. To decrease the analysis time, a second, parallel analytical column could be added to the GC, allowing one column to be used while the other is backflushed. Also, it might be possible to replace the GC with a continuous SF_6 analyzer *(15)*, thus greatly decreasing the time between measurements. The submersible pump could be towed by the boat as part of a computer-controlled instrument package (including CTD and other sensors) allowing a 3-D investigation of tracer distribution in the river.

Acknowledgments

We thank M. Garrison, R. Jacobs, R. Newton, and N. Santella for assistance in the field, B. Huber for processing the CTD data, B. Hales and K. Sullivan for suggestions on the continuous SF_6 system, and F. Hellweger for providing Hudson River geometry data from the Hydroqual model. Many thanks to J. Lipscomb, boat captain of RIVERKEEPER, whose enthusiasm and professionalism made the field work both enjoyable and successful. Hudson River discharge data was obtained from the USGS web site <http://water.usgs.gov>, and Poughkeepsie wind speed data was obtained from NOAA/NCDC. Funding was provided by a generous grant from the Dibner Fund, the Lamont Investment Fund, and by NSF/DOE through the Environmental Molecular Science Institute (EMSI) program (CHE 98-10367). LDEO contribution no. 6317.

Supporting Information Available

Additional information on current model velocity during the experiment as well as Hudson River geometry. This material is available free of charge via the Internet at http://pubs.acs.org.

Literature Cited

(1) Fischer, H. B.; List, E. J.; Imberger, J.; Koh, R. C. Y.; Brooks, N. H. *Mixing in inland and coastal waters*; Academic Press: New York, 1979.
(2) Rutherford, J. C. *River mixing*; John Wiley & Sons: New York, 1994.
(3) O'Connor, D. J. *Int. J. Air Water Pollut.* **1963**, *7*, 1073−1084.
(4) Hetling, L. J.; O'Connell, R. L. *Water Resour. Res.* **1966**, *2*, 825−841.
(5) Hohman, M. S.; Parke, D. B. In *Hudson River Ecology*; Hudson River Valley Commission of New York: Albany, NY, 1969; pp 60−81.
(6) Smart, P. L.; Laidlaw, I. M. S. *Water Resour. Res.* **1977**, *13*, 15−33.
(7) Abidi, S. L. *Water Res. Bull.* **1982**, *16*, 199−204.
(8) Clark, J. F.; Schlosser, P.; Stute, M.; Simpson, H. J. *Environ. Sci. Technol.* **1996**, *30*, 1527−1532.
(9) Clark, J. F.; Schlosser, P.; Simpson, H. J.; Stute, M.; Wanninkhof, R.; Ho, D. T. In *Air−water gas transfer*; Jähne, B., Monahan, E., Eds.; AEON Verlag & Studio: Hanau, Germany, 1995; pp 785−800.
(10) Clark, J. F.; Wanninkhof, R.; Schlosser, P.; Simpson, H. J. *Tellus* **1994**, *46B*, 274−285.
(11) Limburg, K. E.; Moran, M. A.; McDowell, W. H. *The Hudson River Ecosystem*; Springer-Verlag: New York, 1986.
(12) Stedfast, D. A. *Cross sections of the Hudson River estuary from Troy to New York City, New York*; Water-Resources Investigations 80-24; U.S. Geological Survey: 1980.
(13) Flater, D. *Linux J.* **1996**, *32*, 51−57.
(14) Jähne, B.; Munnich, K. O.; Bosinger, R.; Dutzi, A.; Huber, W.; Libner, P. *J. Geophys. Res.* **1987**, *92*, 1937−1949.
(15) Benner, R. L.; Lamb, B. *J. Atmos. Oceanic Technol.* **1985**, *2*, 582−589.

Received for review November 27, 2001. Revised manuscript received April 18, 2002. Accepted April 23, 2002.

ES015814+